scientific reports

Check for updates

OPEN

# Lactoferrin influences atherosclerotic progression by modulating macrophagic AMPK/mTOR signaling-dependent autophagy

Bing Xia[1,2]✉, Jingwei Liang[1,2], Yanlin Lu[1], Jiuyang Ding[1], Jin Peng[1], Fangqin Li[1], Jialin Dai[1], Yubo Liu[1], Jie Wang[1], Changwu Wan[1] & Peng Luo[1]✉

**This study aimed to explore the role of lactoferrin (LTF) in atherosclerosis (AS) and its possible mechanisms. Human left coronary artery tissues were collected and divided into control (CON), coronary heart disease (CHD) and sudden coronary death (SCD) groups. Pathologic changes (including changes in the coronary plaque area, necrotic core, collagen fibers, and foam cell content) were observed. The LTF, P62, and 4-hydroxynonenal (4-HNE) expression levels were assessed. The *ApoE*$^{-/-}$ AS mouse model was established. The pathological changes and related protein levels were analyzed after autophagy inhibition. The foam cell model was constructed using an ox-LDL-induced human monocyte line, THP-1. The LTF, BECN1, LC3-II/I, AMP-activated protein kinase (AMPK)/the mammalian target of rapamycin (mTOR) pathway proteins, B-cell lymphoma-2 (Bcl-2), Bcl-2-associated X protein (Bax), and 4-HNE expressions were then detected after silencing of LTF or BECN1. Plaque stability was significantly lower in the SCD group compared to the non-SCD group ($p < 0.05$). LTF, P62 and 4-HNE levels in plaques increased as plaque stability decreased, and LTF was significantly correlated with plaque progression and autophagy levels. Autophagy inhibition by U0126 leads to the worsening of aortic luminal stenosis, increased necrotic core and foam cell deposits, decreased autophagosomes, reduced LTF expression, and upregulated P62 expression in AS mice. It was further demonstrated that LTF expression correlates with autophagy. LTF expression was increased in ox-LDL-treated THP-1 cells, and silencing BECN1 and/or LTF increased mTOR phosphorylation and 4-HNE levels, inhibited BECN1 and LC3 II expression and AMPK activation, and simultaneously decreased the Bcl-2/Bax ratio. LTF might alleviate AS pathology through accelerating the AMPK/mTOR pathway, and suggested that LTF may be a potential predictive molecule for AS.**

**Keywords** Lactoferrin, Atherosclerosis, Sudden coronary death, Autophagy, AMPK, mTOR

The prevalence of cardiovascular diseases is on the rise with each passing year among non-communicable diseases worldwide[1]. Of these, CHD accounts for about one-third of cardiovascular diseases, and sudden death is the most severe complication of CHD. According to statistics, about 20% of patients with cardiovascular disease succumb to SCD each year[2]. Early clinical prediction and diagnosis are prioritized in the prevention and treatment of SCD due to the extremely rapid onset of SCD and its low survival rate[3,4]. AS is an important pathological basis for most cardiovascular diseases, including CHD. Macrophage phagocytosis of lipid droplets induces an inflammatory response leading to atherogenesis. Macrophage death (autophagy and apoptosis) and oxidative stress influence AS processes[5–7]. However, AS pathogenesis is intricate, and the precise mechanisms contributing to its development are unclear. Consequently, it is crucial to elucidate the mechanisms that affect the AS process to prevent and treat SCD.

LTF is an iron transport protein, mainly secreted by neutrophils, and possesses anti-inflammatory, antioxidant, and antifibrotic properties[8–10]. For instance, a study demonstrated that LTF inhibits apoptosis caused by oxidative stress[11]. It has also been demonstrated that LTF improves myocardial fibrosis and myocardial remodeling after

[1]School of Forensic Medicine, Guizhou Medical University, Guiyang 550004, Guizhou, China. [2]Bing Xia and Jingwei Liang contributed equally to this work. ✉email: 372732293@qq.com; 519484547@qq.com

myocardial infarction[9]. The AS in mice on a high-fat diet were alleviated by LTF supplementation, which increased cholesterol excretion[12]. Our previous study also confirmed that aberrant methylation of the promoter region of the LTF gene occurs in the coronary artery tissues of individuals who died suddenly from CHD[13], suggesting that LTF is closely linked to AS.

Many recent studies have demonstrated that autophagy, apoptosis, and oxidative stress play important roles in AS[14–17]. It has been discovered that enhanced autophagy can reduce intracellular lipid deposition and inhibit foam cell formation, thereby slowing down the AS[18]. Several molecules fulfill critical functions in the autophagy process. For instance, protein 1 light chain 3 (LC3) is involved in the formation of autophagosomes and is frequently employed as a biomarker of autophagy[19]. As one of the key molecules of autophagy, BECN-1 also plays a critical role in autophagy regulation[20]. The AMPK/mTOR is an upstream signaling regulatory pathway for autophagy. An increased AMP/ATP ratio activates AMPK, inhibiting mTOR activation and ultimately activating autophagy[21,22]. Apoptosis and oxidative stress in the vasculature are involved in the AS and associated with AMPK activation. The B-cell lymphoma-2 (Bcl-2)/Bcl-2-associated X protein (Bax) ratio can be implemented to assess the degree of apoptosis. AMPK Activation reduces apoptosis by decreasing the Bcl-2/Bax ratio[23]. 4-hydroxynonenal (4-HNE) is a marker of oxidative stress. Activation of AMPK decreases 4-HNE to prevent cellular damage. Activation of AMPK decreases 4-HNE content to avoid cell damage[24].

Furthermore, LTF can activate cellular autophagy through the AMPK/mTOR signaling pathway[11]. Additionally, LTF inhibits apoptosis and oxidative stress[25,26]. Therefore, the objective of the current investigation was to determine whether LTF can influence macrophage death by modulating autophagy through the activity of the AMPK/mTOR signaling pathway, which is implicated in the AS.

## Materials and methods

### Study participants

Tissues of the left anterior descending branch of the coronary artery were collected from autopsies performed at the Guizhou Medical University Forensic Judicial Identification Centre from January 1, 2021 to December 1, 2023 for storage at -80 °C. Inclusion criteria for the control group ($n=6$) were as follows: (1) Accidental death determined at autopsy, and pathological examination concluded that they did not have any cardiac disease or AS, and (2) autopsy was performed within 24 h of death. Inclusion criteria for the disease group were as follows: (1) Autopsy subjects with CHD; (2) the presence of significant plaque in the lumen of the left anterior descending branch of the coronary artery; (3) luminal stenosis of ≥ 50%; (4) autopsy within 24 h of death. The coronary tissue of individuals identified in forensic pathology was categorized into the SCD group ($n=6$) and the CHD group ($n=6$).

The exclusion criteria were as follows: (1) Coronary tissues that have expired more than 24 h, exhibiting tissue decay, autolysis, and unclear structure; (2) the coronary tissues of individuals who expired due to other types of heart diseases, such as myocarditis and rheumatic heart disease; (3) the coronary tissues of the individual who deceased due to drug abuse.

This study is in line with the rules contained in the Declaration of Helsinki. The informed consent were verbally informed to the patients' immediate family members, two or more family members, the public security authorities, and two qualified forensic pathologists from our organization witnessed the event. All participants' personal information was anonymized. This study was approved by the Ethics Committee of Guizhou Medical University (ethical approval number: 2024–112), and the ethics committee waived the requirement for informed consent.

### Animal experimentation

C57BL/6 and its background *ApoE*$^{-/-}$ mice (eight weeks old) were acquired from Guizhou Medical University Animal Centre. All mice were housed at 24–25 °C with 55% humidity, 12 h light and 12 h dark, food and water available ad libitum. All mice treated in this study were reported in accordance with the ARRIVE guidelines and that all methods were performed in accordance with its relevant guidelines and regulations.

C57BL/6 mice were the control (CON) mice. After one week of acclimatization feeding, all *ApoE*$^{-/-}$ mice were randomly assigned to one of two groups (eight mice per group). They were provided with a high-fat diet (3% cholesterol, 0.2% propylthiouracil, 0.5% sodium cholate, 10% lard, 5% sugar, and 81.3% base feed) for 14 weeks. After 8 weeks of rearing on a high-fat diet, saline (once every three days) was administered in the AS group, and the U0126 inhibitor[27,28] (5 μg/10 μL, once every three days) was given to the U0126 group via the tail vein. After four weeks of continuous injections, all mice were euthanized directly by intraperitoneal injection of sodium pentobarbital (80 mg/kg), and then dissected, and the hearts and aortas were collected and fixed in 4% paraformaldehyde. This study was approved by the Animal Ethics Committee of Guizhou Medical Universit (approval number 2402125).

### Cell culture

THP-1 cell line was purchased from Shanghai FHS Biotechnology Co. Ltd. (Shanghai, China). The cells were cultured in RPMI-1640 medium supplemented with 10% fetal bovine serum at 37 °C and 5% $CO_2$. THP-1 cells were induced with 160 nM phorbol 12-myristate 13-acetate (PMA) for 48 h and then exposed to ox-LDL (100 μg/mL) and incubated together for 24 h. The cells were transiently transfected with LTF and BECN1 si-RNA (RiboBio, China). Silencing efficiency was assessed by immunoblotting.

### Immunoblotting

The total protein extraction from human coronary tissues and cell lysates was conducted using Radio immunoprecipitation assay lysis buffer containing Phenylmethanesulfonyl fluoride and phosphatase inhibitors. Sodium dodecyl-sulfate polyacrylamide gel electrophoresis was employed to separate the proteins of each

sample, which were subsequently transferred to a polyvinylidene difluoride membrane (Millipore, USA). The membranes were closed in skimmed milk for 2 h and subsequently incubated with LTF (Cat # ET7109-95, HUABIO, China), AMPK (Cat # R23314, ZENBIO, China), p-AMPK (Cat # 381164, ZENBIO, China), mTOR (Cat # 67778 -1-lg, Proteintech, China), p-mTOR (Cat # 67778-l-lg, Proteintech, China), BECN1 (Cat # 11306-1-AP, Proteintech, China), P62 (Cat # 18420-1-AP, Proteintech, China), LC3B (Cat: No18725-1-AP, Proteintech, China), 4HNE (Cat # MAB3249, R&D systems, America), Bax (Cat # ER0907, HUABIO, China) (concentration 1:1000), Bcl-2 (Cat # ET1702-53, 1:2000, HUABIO, China), β-Actin (Cat #EM2-1002, 1:5000, HUABIO, China) at 4 °C overnight. The membranes were incubated for 2 h at room temperature (RT) in the presence of horseradish peroxidase (HRP)-conjugated secondary antibody (1:5000). After visualization of the bands using an enhanced chemiluminescent liquid, they were detected in a chemiluminescence imaging system (BIO-RAD). Quantifying protein bands using ImageJ software (Version 2.0, https://imagej.net/, National Institutes of Health). All original blots were included in Supplementary file (Supporting Information).

### Histopathological and immunohistochemical (IHC) staining

After fixation with 4% paraformaldehyde, vascular tissues were made into sections of 5 μm thickness, which were then subjected to hematoxylin-eosin (HE), Masson trichrome, and Movat staining, respectively. Coronary plaque area, necrotic core, collagen fiber content, and foam cell counts were observed under light microscopy. Paraffin sections were incubated overnight with antibodies against LTF (Cat # ET7109-95, HUABIO, China), BECN-1 (Cat # 11306-1-AP, Proteintech, China), P62 (Cat # 18420-1-AP, Proteintech, China), and 4-HNE (Cat # MAB3249, R&D Systems, America) (1:200 dilution), respectively. Subsequently, tissue sections were incubated with (HRP)-labeled anti-rabbit or anti-mouse IgG secondary antibodies for 2 h. The 3,3'-Diaminobenzidine was used to visualize positive immunoreactivity. Quantitative analysis of all pathology images from the sample was performed using ImageJ software.

### Immunofluorescence (IF) staining

The prepared sections were routinely dewaxed, hydrated, and incubated with peroxidase for 10 min at RT, washed three times with phosphate-buffered saline and digested with complex enzymes for 30 min, and closed with goat serum and then given a primary antibody LTF to be incubated with CD68 (1:100 dilution, Cat # 28058-l-AP, Gene Tex, China) respectively overnight at 4 °C, and then with a secondary antibody (1:200 dilution, Cat # ET7109-95, HUABIO, China) for 1 h at RT, and analyzed for the LTF (green light) and CD68 (red light) in AS. Images were acquired using an inverted fluorescence microscope (DMi8, Leica, Germany).

### TdT-mediated dUTP nick end labeling (TUNEL) staining

Apoptosis of treated THP-1 cells was detected using the Tunel apoptosis detection kit (Cat # C1088, Beyotime, Nanjing, China). According to the manufacturer's instructions, apoptosis was determined using the one-step Tunel apoptosis detection kit. Images were acquired using an inverted fluorescence microscope (DMi8, Leica, Germany).

### Transmission electron microscopy (TEM)

Mice aorta were pre-fixed with 3% glutaraldehyde, re-fixed with 1% osmium tetroxide, dehydrated step by step with acetone, embedded with Epon812, semi-thin sections were stained with toluidine blue for optical localization, and ultrathin sections were made with a diamond knife and stained with uranyl acetate and lead citrate for TEM observation by JEM-1400FLASH.

### Statistical analysis

All data are expressed as mean (M) ± standard error of the M. Statistical analysis was performed using Statistical Package for the Social Sciences software (version 22.0; http://www.spss.com.hk/, IBM, New York, USA), and graphs were prepared using GraphPad Prism software (version 10.0; https://www.graphpad.com/, California, USA). Comparisons between groups were made using a one-way analysis of variance by Bonferrnoi's *post hoc*. A $p < 0.05$ was considered statistically significant.

## Results

### LTF expression is upregulated in coronary atherosclerotic plaques

The HE, Movat, and Masson staining were used to analyze the plaque area, necrotic core, number of foam cells, and collagen fiber content in 18 cases of coronary artery tissue. HE staining demonstrated that the vessel wall in the CON group was smooth, and the intima was flat, continuous, and well-arranged. Compared to the CON group, the intima in the disease group was thickened, ruptured, and structurally disorganized, with the intima protruding into the lumen to form a fibrous cap, and the lumen of the vessel was significantly narrowed ($p < 0.05$). The area of necrotic cores and plaques in the SCD group was enlarged and significantly higher than in the CHD group ($p < 0.05$) (Fig. 1A, F, and G). Movat staining depicted disorganization of the intima-media structure of the vessel wall of the coronary tissue in the disease group, with ruptured continuity and increased foam cells (Fig. 1B and H). Masson staining exhibited a significant increase in collagen fibers within the fibrous cap in the CHD group compared to the CON group ($p < 0.05$). In the SCD group, as the disease worsened, the collagen fiber and collagen content within the fibrous cap were significantly reduced compared to CHD and CON groups, and plaque stability decreased ($p < 0.05$) (Fig. 1C and I). We subsequently detected LTF expression in human coronary artery samples by immunoblotting and IHC. Notably, the results revealed that LTF expression was upregulated in coronary arteries with plaque compared with those without plaque ($p < 0.05$) (Fig. 1D, E, J, and K), and that LTF was predominantly distributed within the cytoplasm of foam cell cytoplasm, demonstrating the potential of LTF as a biomarker for CHD. Additionally, immunofluorescence co-localization revealed that LTF

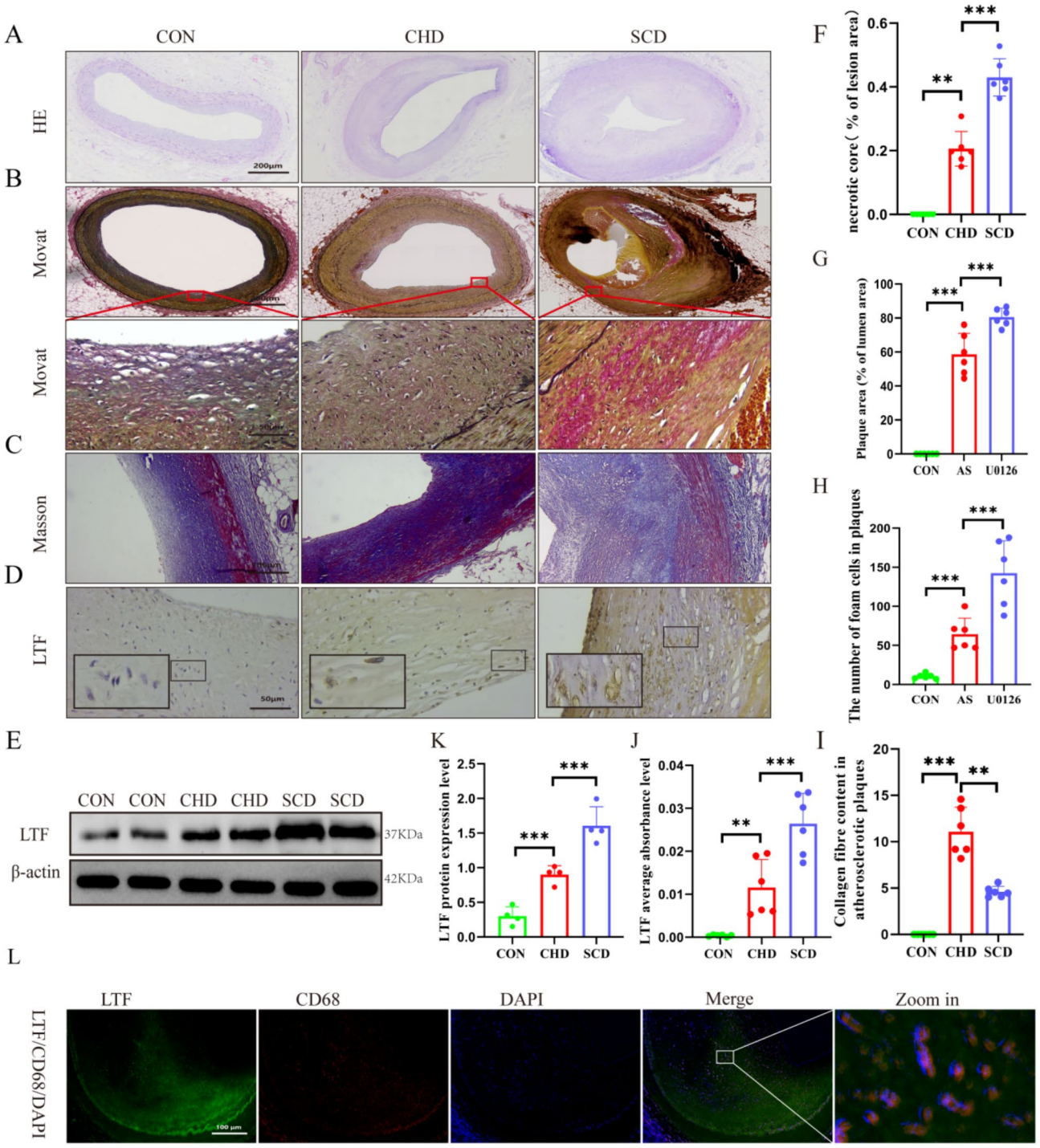


**Fig. 1**. Changes in LTF expression in coronary atherosclerotic plaques. (**A**–**C**) HE staining of the left anterior descending branch of a human coronary artery (magnification, 10×), MOVAT, and Masson staining (magnification, 40×). (**D** and **J**) IHC analysis of LTF expression and its semi-quantitative analysis. (**E** and **K**) Immunoblotting detected the expression of LTF and its semi-quantitative analysis. (**F**–**I**) Quantitative analysis of necrotic core, plaque area, foam cell count, and collagen fiber content. (**L**) IF co-localization of LTF and CD68 in atherosclerotic plaques. $^{**}p < 0.01$, and $^{***}p < 0.001$ ($n = 4$ or 6 samples each group).

co-localized with the macrophage marker CD68 in human coronary arteries (Fig. 1L). This further suggesting that LTF is expressed in macrophages. Therefore, we will select THP-1 cells to investigate the LTF mechanism in CHD further.

### Autophagy and oxidative stress levels in human coronary artery tissue

Additionally, we detected the expression of P62, BECN1, and 4-HNE in human coronary atherosclerotic plaques by immunoblotting and IHC. We discovered that P62 and 4-HNE expression was upregulated, and BECN1 expression was reduced in the CHD group compared to the CON group, and this change was more pronounced in the SCD group ($p < 0.05$) (Fig. 2). Suggesting that as the disease progresses, the level of autophagy within the plaque decreases and the level of oxidative stress increases.

### Correlation analysis of LTF with coronary plaque structural and autophagy indices and oxidative stress markers

Correlations between LTF expression and plaque area ratio, necrotic core, the number of foam cells and collagen fiber content were examined using the Pearson correlation coefficient to explore the relationship between LTF

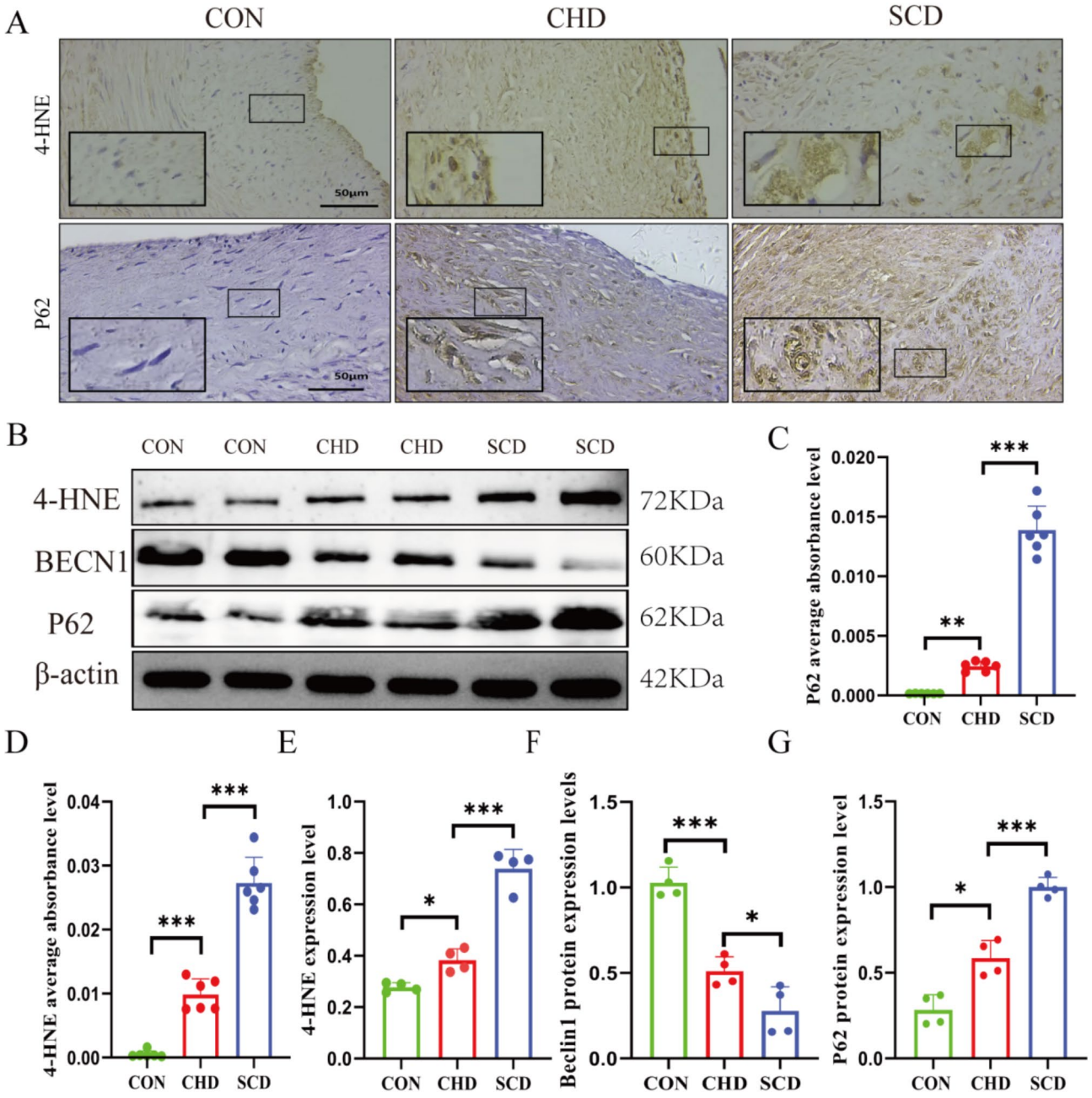


**Fig. 2**. Expression of BECN1, P62 and 4-HNE detected by IHC and immunoblotting and their quantitative analysis. $^{*}p < 0.05$, $^{**}p < 0.01$, and $^{***}p < 0.001$ ($n = 4$ or 6 samples each group).

expression and plaque stability. The results indicated that LTF expression positively correlated with necrotic core, plaque area ratio, and macrophage-derived foam cells within the plaque ($p < 0.05$). However, there was no correlation between LTF and collagen fiber content ($p > 0.05$). To further analyze the relationship between LTF expression and autophagy and oxidative stress in coronary atherosclerotic plaques, correlations between LTF and P62, BECN1, and 4-HNE were examined using Pearson correlation coefficients. The results exhibited that in coronary AS, the expression of LTF was positively correlated with the expression of P62 and 4-HNE and negatively correlated with the expression of BECN1 ($p < 0.05$) (Fig. 3). Accordingly, a significant correlation existed between LTF expression autophagy and oxidative stress.

## Changes in LTF expression in mice after Inhibition of autophagy

We observed necrotic cores, plaque area ratio, and foam cell counts in aortic plaques of *ApoE*$^{-/-}$ mice using HE and Movat stainings to investigate the role of LTF in vivo. Additionally, we evaluated the expression and autophagy levels of LTF in the mice aorta by IHC and TEM. U0126 is an autophagy inhibitor that reduces ischemia/reperfusion-induced autophagy in myocardium[29]. HE staining revealed AS in *ApoE*$^{-/-}$ mice on a high-fat diet developed atherosclerotic plaques, indicating that the atherosclerosis mouse model was successfully constructed. And compared with the AS group, aortic plaques and necrotic core areas were further increased in atherosclerotic mice after inhibition of autophagy by U0126. ($p < 0.05$) (Fig. 4A and F-G). Movat staining revealed an increase in foam cells within the atherosclerotic plaques of mice in the U0126 group ($p < 0.05$) (Fig. 4B and H). In addition, TEM revealed a significant reduction of autophagosomes in the aorta of the U012 group compared to the AS group ($p < 0.05$) (Fig. 4C). Furthermore, IHC revealed a significant increase in LTF and P62 expression in the plaques of the *ApoE*$^{-/-}$ mice relative to the C57BL/6 mice and a decrease in LTF expression and an increase in P62 expression after inhibition of autophagy in vivo in the mice ($p < 0.05$) (Fig. 4D-E and I-J), suggesting that autophagy levels influence LTF expression.

## LTF induces autophagy in THP-1 cells through the AMPK/mTOR pathway

Macrophage phagocytosis of lipids to form foam cells is a central factor in the development of AS. In some cases, macrophages can reduce foam cell formation by eliminating ox-LDL through autophagy. Oil red O (ORO) was conducted following the silencing of LTF using small interfering (si)-RNA to ascertain the impact of LTF on the transformation of THP-1 cells to foam cells and on lipid uptake in THP-1 cells. The results exhibited a significant increase in lipid uptake in THP-1 cells after stimulation with a risk factor (ox-LDL) and a further increase in intracellular lipid deposition after silencing LTF ($p < 0.05$) (Fig. 5A, B). Moreover, IF results exhibited a decreased LTF expression after silencing LTF and BECN1 ($p < 0.05$) (Fig. 5A and C-D); it was found by immunoblotting that the levels of BECN1 and LC3 II in macrophages were significantly reduced, and P62 expression was increased in cells after silencing LTF. Similarly, LTF, BECN1, and LC3 II expression were down-regulated and P62 expression was increased after silencing BECN1 ($p < 0.05$) (Fig. 5E–K). Activation of AMPK and inhibition of mTOR can induce autophagy. Upon silencing LTF or BECN1, AMPK phosphorylation was inhibited, and

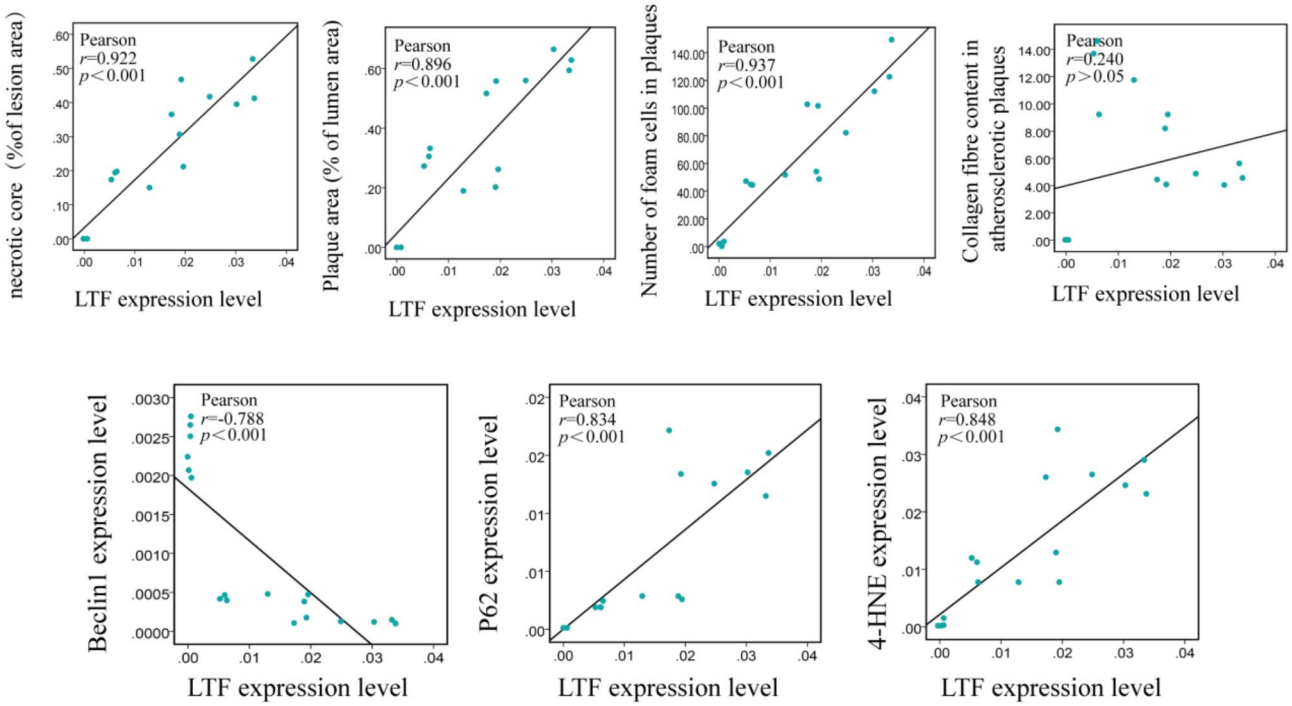


**Fig. 3**. Correlation analysis of LTF with necrotic core, plaque area, foam cell count, collagen fiber content, 4-HNE, P62, and BECN1.

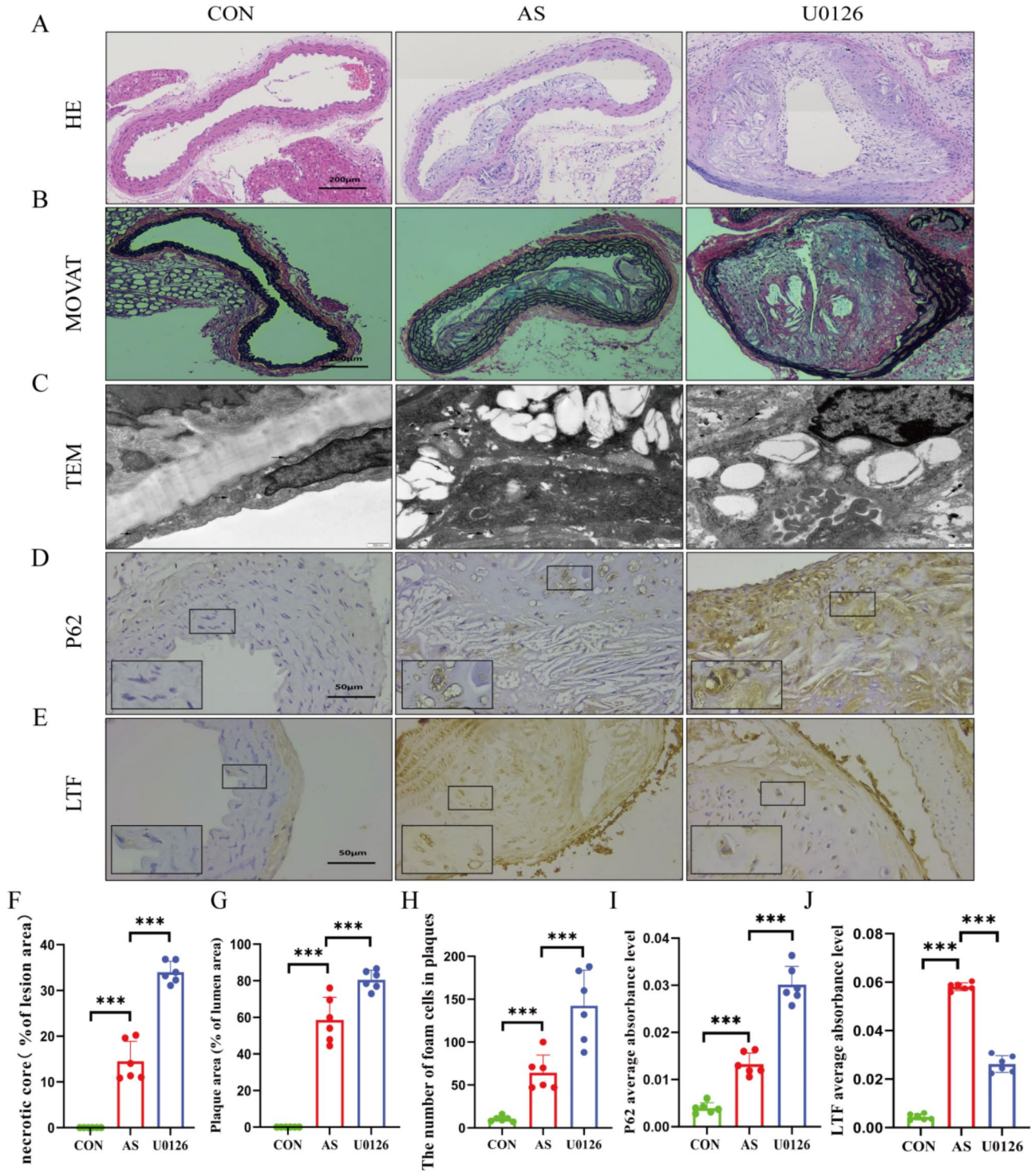


**Fig. 4**. Changes in LTF and autophagy levels in mice aorta. (**A**,**B**) Representative pictures of HE and MOVAT stainings of mice aorta (magnification, 10×). (**C**) TEM observation of autophagosomes (arrow) within mice aorta. (**D**,**E**) IHC observation of LTF and P62 expression and localization (magnification, 40×). (**F**–**H**) Necrotic core, plaque area ratio, and foam cell counts in mice aorta. (**I**,**J**) Quantitative analysis of P62 and LTF in mice aorta by IHC. ***$p < 0.001$ (Each group $n = 6$).

mTOR phosphorylation was activated ($p < 0.05$) (Fig. 5E and I-J). These findings suggest that silencing LTF expression inhibits autophagy by suppressing AMPK and activating the mTOR pathway.

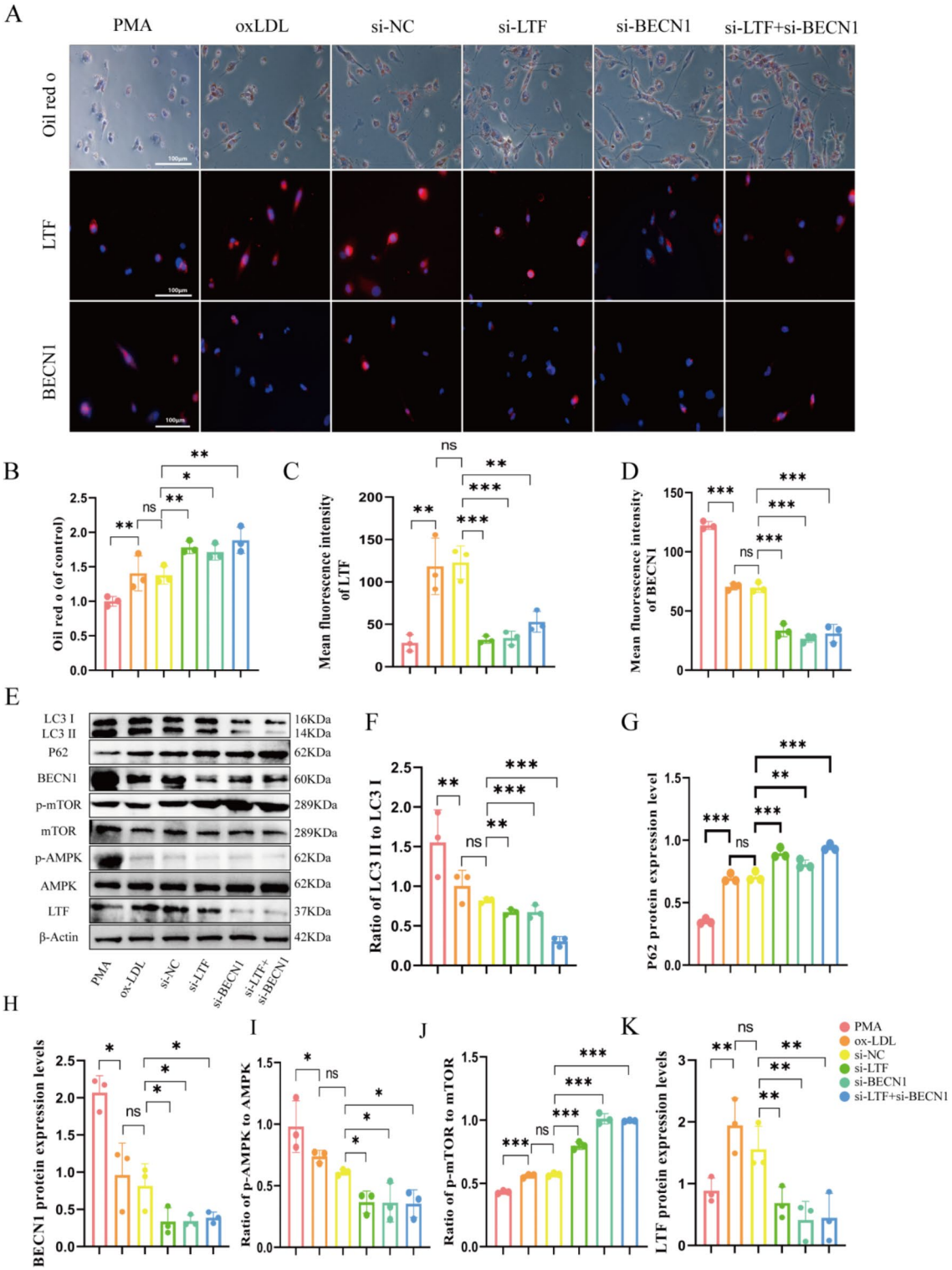


**Fig. 5**. Inhibition of LTF could inhibit autophagy through the AMPK/mTOR pathway. (**A**–**D**) Observation and quantification of intracellular lipid deposition by ORO, and IF localization and quantification of intracellular LTF and BECN1. (**E**–**K**) Immunoblotting detected the expression level and quantitative analysis of AMPK/mTOR pathway proteins and LTF, BECN1, P62 and LC3B proteins. $^{*}p < 0.05$, $^{**}p < 0.01$, and $^{***}p < 0.001$ (Each group $n = 3$).

### LTF inhibits oxidative stress and apoptosis by enhancing autophagy in THP-1 cells

We explored the role of LTF on cellular oxidative stress and apoptosis, considering the important role of macrophage survival in AS. We analyzed the expression of oxidative stress and apoptosis-associated proteins, including 4-HNE, Bax, and Bcl2, by immunoblotting after the LTF and BECN1 were specifically knocked down by si-RNA. The results revealed a significant increase in the oxidative stress product 4-HNE and a significant decrease in the Bcl-2/Bax ratio upon inhibition of LTF ($p < 0.05$). The same results were attained when BECN1 was silenced to inhibit autophagy (Figs. 6A–C). The Tunel assay detected increased apoptosis after silencing LTF and BECN1 (Fig. 6D-E). These results suggest that LTF can inhibit cellular oxidative stress and apoptosis by enhancing autophagy.

## Discussion

The present investigation revealed an increase in LTF expression with the progression of atherosclerotic plaques. In vivo experiments further demonstrated that LTF was detected within the plaques of mice after fed a high-fat diet. However, there was a relative decrease in the expression of LTF as the aortic plaque area increased upon the inhibition of their autophagy. These findings suggest that LTF may be involved in the atherosclerotic process via the autophagy pathway. Furthermore, we have demonstrated in in vitro experiments that LTF defects in macrophages exacerbate AS by inhibiting autophagic flux through the AMPK/mTOR signaling pathway.

A previous study found that LTF levels in the blood correlate with the degree of coronary artery stenosis[30]. Exogenous LTF supplementation improves cholesterol metabolism and alleviates AS pathology in *ApoE*$^{-/-}$ mice[12]. Our study found that high levels of LTF was detected in coronary atherosclerotic plaques of SCD patients. A number of studies have shown that anti-inflammatory factors promote vascular inflammation, increase the risk of intraplaque hemorrhage, and promote inflammatory cell infiltration to destabilize coronary plaques, and that an increase in anti-inflammatory factors leads to an inflammatory imbalance that exacerbates atherosclerosis[31–33]. Therefore, in our study, this may have contributed to the increased expression of LTF within atherosclerotic plaques. Besides, we found that P62 and 4-HNE expression were increased and Beclin1 expression was decreased during plaque progression. In addition, a correlation between LTF expression and plaque area, autophagic flux and oxidative stress levels were observed. Those results suggests that LTF might be an effective biomarker for the diagnosis of SCD. Meanwhile, we further found that inhibiting autophagy significantly reduced LTF levels in mice plaques. Anti-inflammatory factors induce cellular autophagy[34]. Similarly, in the case of defective autophagy, there is a corresponding reduction in the decreased secretion of anti-inflammatory factors[35]. This may account for the reduced expression of LTF with anti-inflammatory effects after inhibition of atherosclerosis in mice. These observations suggest that LTF expression is influenced by autophagy levels.

A variety of cells, such as macrophages, vascular smooth muscle cells, and vascular endothelial cells, are involved in the development of AS. Previous studies have shown that lactoferrin strongly inhibits cholesterol accumulation in VSMC by affecting binding to agLDL[36]. At the same time, lactoferrin can be involved in the protection of vascular endothelial cells from oxidative damage by regulating the PI3K/AKT/ERK1/2 pathway[37]. Most of the current studies have focused on exogenous lactoferrin exerting effects on AS. However, at the molecular level, the mechanism of action by which LTF affects the course of AS by regulating macrophages is unclear. We found that LTF co-localized with the macrophage marker CD68 by immunofluorescence co-localization staining. This suggests that LTF is expressed intracellularly in macrophages. Therefore, we will explore the mechanism of LTF action in macrophages.

Foam cell formation is the initiation of atherosclerotic formation and is influenced by autophagy levels[6,38]. Activation of AMPK inhibits mTOR phosphorylation to initiate autophagy. Increasing AMPK activity will reduce foam cell formation and protect against AS[39,40]. Previous studies have revealed that LTF can activate AMPK and inhibit mTOR[11]. To further explore the role of LTF on the AMPK/mTOR signaling pathway, we first constructed a foam cell model by THP-1 cells. Subsequently, we employed si-RNA to silence LTF and silencing BECN1 to inhibit autophagy. We observed a significant increase in intracellular lipid deposition after inhibiting LTF and autophagy. Previous research had demonstrated that ox-LDL generates an inflammatory response when it induces the conversion of macrophages to foam cells[41]. LTF is released into the plasma to combat inflammation and infection[30]. Our observation that LTF expression is upregulated following ox-LDL induction implies that LTF expression is being increased to combat the inflammatory response. Furthermore, we analyzed the phosphorylated levels of AMPK and mTOR proteins in THP-1 cells and assessed the expression levels of autophagy-associated proteins P62, BECN1 and LC3B. LTF expression decreased significantly following the silencing of either LTF or BECN1. The inhibition of LTF significantly decreased the level of AMPK phosphorylation and increased the activation of mTOR. Concurrently, the expression of autophagic protein BECN1 and the LC3II/ I ratio were both significantly reduced, and P62 expression was increased. These results further confirm that inhibition of LTF may result in impaired autophagic flux, reducing the formation of macrophage-derived foam cells.

The AMPK/mTOR signaling pathway regulates macrophage apoptosis and oxidative stress[42,43]. Previous studies had depicted that AMPK can induce anti-apoptotic effects by increasing the Bcl-2/Bax ratio[44]. In our in vitro study, silencing LTF and/or inhibition of autophagy significantly reduced both AMPK activation and the Bcl-2/Bax ratio. Reactive oxygen species, the second messenger, regulate AMPK activation through positive feedback and are common mediators of cardiovascular risk factor pathogenicity[45]. We observed an increase in the oxidative stress product 4-HNE following the knockdown of LTF and BECN1. These findings suggested that LTF inhibition increases apoptosis and oxidative stress. Our study confirms that LTF can attenuate apoptosis and oxidative stress by regulating autophagy through the AMPK/mTOR signaling pathway, thereby alleviating the AS. However, the mechanism has not been deeply explored in mice models, and the role of LTF overexpression should be verified in subsequent experiments.

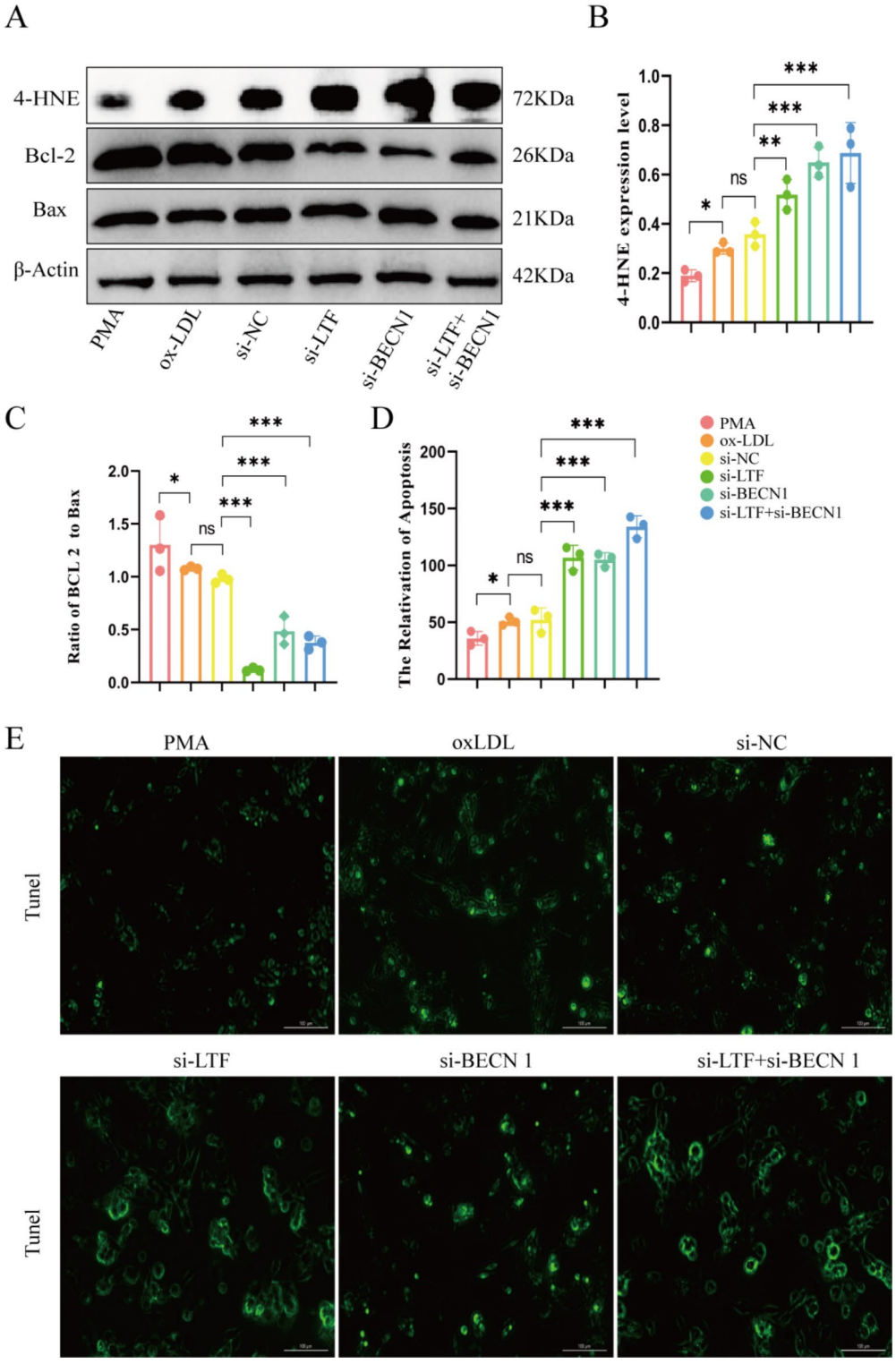


**Fig. 6**. Inhibition of LTF enhances apoptosis and oxidative stress. (**A**–**C**) immunoblotting detection of Bax, Bcl-2, and 4-HNE expression levels, and quantitative analysis. (**D**-**E**). Detection of apoptosis by Tunel staining and its quantitative analysis (magnification, 20×). $^{*}p < 0.05$, $^{**}p < 0.01$, and $^{***}p < 0.001$. (Each group $n = 3$).

Our results suggested that LTF is a potential biomarker of AS, and it effectively reduced ox-LDL-induced macrophage-derived foam cell formation, lipid accumulation, and cell decath. Furthermore, LTF regulated AMPK activation, oxidative stress, and apoptosis. LTF regulated autophagic flux through the AMPK/mTOR pathway and inhibited foam cell oxidative stress and apoptosis levels, alleviating the atherosclerotic process (Fig. 7).

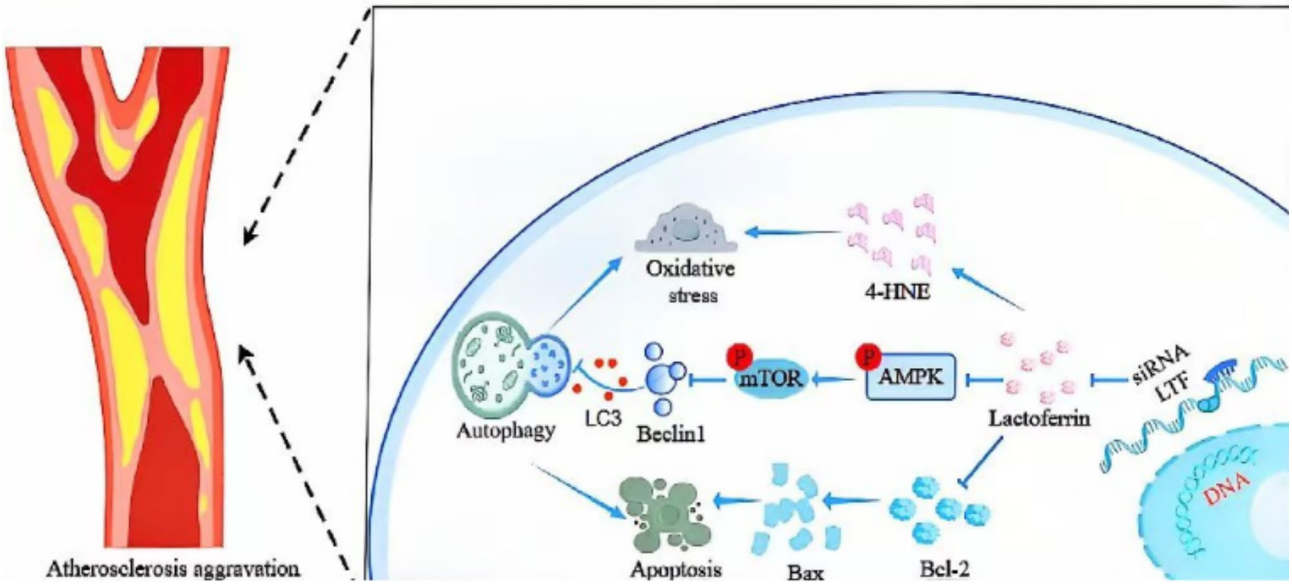


**Fig. 7**. Diagram of the mechanism of LTF involvement in atherosclerosis.

## Data availability

The raw data supporting the conclusions of this article will be made available by the authors without reservation. And the raw data are available from the corresponding author upon request.

Received: 17 January 2025; Accepted: 19 March 2025
Published online: 27 March 2025

## References

1. Tsao, C. W. et al. Heart disease and stroke statistics-2022 update: A report from the American heart association. *Circulation* **145**, e153–e639. https://doi.org/10.1161/CIR.0000000000001052 (2022).
2. Wong, C. X. et al. Epidemiology of sudden cardiac death: global and regional perspectives. *Heart Lung Circ.* **28**. https://doi.org/10.1016/j.hlc.2018.08.026 (2019).
3. Li, Y. et al. Risk prediction for sudden cardiac death in the general population: A systematic review and meta-analysis. *Int. J. Public. Health* **69**, 1606913. https://doi.org/10.3389/ijph.2024.1606913 (2024).
4. Park, S. J. et al. Preventive percutaneous coronary intervention versus optimal medical therapy alone for the treatment of vulnerable atherosclerotic coronary plaques (PREVENT): a multicentre, open-label, randomised controlled trial. *Lancet* **403**, 1753–1765. https://doi.org/10.1016/S0140-6736(24)00413-6 (2024).
5. De Meyer, G. R. Y., Zurek, M., Puylaert, P. & Martinet, W. Programmed death of macrophages in atherosclerosis: mechanisms and therapeutic targets. *Nat. Rev. Cardiol.* **21**, 312–325. https://doi.org/10.1038/s41569-023-00957-0 (2024).
6. Qiao, L. et al. Deficient chaperone-mediated autophagy promotes inflammation and atherosclerosis. *Circ. Res.* **129**, 1141–1157. https://doi.org/10.1161/CIRCRESAHA.121.318908 (2021).
7. Cheng, C. et al. NPRC deletion mitigated atherosclerosis by inhibiting oxidative stress, inflammation and apoptosis in ApoE knockout mice. *Signal. Transduct. Target. Ther.* **8**, 290. https://doi.org/10.1038/s41392-023-01560-y (2023).
8. Wang, B., Timilsena, Y. P., Blanch, E., Adhikari, B. & Lactoferrin Structure, function, denaturation and digestion. *Crit. Rev. Food Sci. Nutr.* **59**, 580–596. https://doi.org/10.1080/10408398.2017.1381583 (2019).
9. Ye, T. et al. Lactoferrin attenuates cardiac fibrosis and cardiac remodeling after myocardial infarction via inhibiting mTORC1/S6K signaling pathway. *Theranostics* **13**, 3419–3433. https://doi.org/10.7150/thno.85361 (2023).
10. Hu, P. et al. Lactoferrin relieves deoxynivalenol-induced oxidative stress and inflammatory response by modulating the Nrf2/MAPK pathways in the liver. *J. Agric. Food Chem.* **71**, 8182–8191. https://doi.org/10.1021/acs.jafc.3c01035 (2023).
11. Hsu, Y. H. et al. Lactoferrin contributes a renoprotective effect in acute kidney injury and early renal fibrosis. *Pharmaceutics* **12**. https://doi.org/10.3390/pharmaceutics12050434 (2020).
12. Ling, C. J. et al. Lactoferrin alleviates the progression of atherosclerosis in ApoE-/- mice fed with high-fat/cholesterol diet through cholesterol homeostasis. *J. Med. Food.* **22**, 1000–1008. https://doi.org/10.1089/jmf.2018.4389 (2019).
13. Xia, B. et al. Association of GAL-8 promoter methylation levels with coronary plaque inflammation. *Int. J. Cardiol.* **401**, 131782. https://doi.org/10.1016/j.ijcard.2024.131782 (2024).
14. Klionsky, D. J. et al. Autophagy in major human diseases. *EMBO J.* **40**, e108863. https://doi.org/10.15252/embj.2021108863 (2021).
15. Fang, S. et al. IRGM/Irgm1 facilitates macrophage apoptosis through ROS generation and MAPK signal transduction: Irgm1+/- mice display increases atherosclerotic plaque stability. *Theranostics* **11**, 9358–9375. https://doi.org/10.7150/thno.62797 (2021).
16. Jeong, S. J., Zhang, X., Rodriguez-Velez, A., Evans, T. D. & Razani, B. p62/SQSTM1 and selective autophagy in cardiometabolic diseases. *Antioxid. Redox Signal.* **31**, 458–471. https://doi.org/10.1089/ars.2018.7649 (2019).
17. Batty, M., Bennett, M. R. & Yu, E. The role of oxidative stress in atherosclerosis. *Cells* **11**. https://doi.org/10.3390/cells11233843 (2022).
18. Zhao, Y. et al. Deacetylation of Caveolin-1 by Sirt6 induces autophagy and retards high glucose-stimulated LDL transcytosis and atherosclerosis formation. *Metabolism* **131**, 155162. https://doi.org/10.1016/j.metabol.2022.155162 (2022).
19. Shang, J. N. et al. The nonautophagic functions of autophagy-related proteins. *Autophagy* **20**, 720–734. https://doi.org/10.1080/15548627.2023.2254664 (2024).
20. Prerna, K. & Dubey, V. K. Beclin1-mediated interplay between autophagy and apoptosis: new Understanding. *Int. J. Biol. Macromol.* **204**, 258–273. https://doi.org/10.1016/j.ijbiomac.2022.02.005 (2022).

21. Steinberg, G. R. & Hardie, D. G. New insights into activation and function of the AMPK. *Nat. Rev. Mol. Cell. Biol.* **24**, 255–272. https://doi.org/10.1038/s41580-022-00547-x (2023).
22. Owaki, R. et al. AMPK activators suppress cholesterol accumulation in macrophages via suppression of the mTOR pathway. *Exp. Cell. Res.* **432**, 113784. https://doi.org/10.1016/j.yexcr.2023.113784 (2023).
23. Wu, Y. Metformin inhibits mitochondrial dysfunction and apoptosis in cardiomyocytes induced by high glucose via upregulating AMPK activity. *Exp. Biol. Med. (Maywood)* **248**, 1556–1565. https://doi.org/10.1177/15353702231191178 (2023).
24. Zhang, Y. et al. Sulforaphane alleviates high fat diet-induced insulin resistance via AMPK/Nrf2/GPx4 axis. *Biomed. Pharmacother.* **152**, 113273. https://doi.org/10.1016/j.biopha.2022.113273 (2022).
25. Liu, H. et al. Lactoferrin protects against iron dysregulation, oxidative stress, and apoptosis in 1-methyl-4-phenyl-1,2,3,6-tetrahydropyridine (MPTP)-induced Parkinson's disease in mice. *J. Neurochem.* **152**, 397–415. https://doi.org/10.1111/jnc.14857 (2020).
26. He, H. et al. Lactoferrin alleviates spermatogenesis dysfunction caused by bisphenol A and cadmium via ameliorating disordered autophagy, apoptosis and oxidative stress. *Int. J. Biol. Macromol.* **222**, 1048–1062. https://doi.org/10.1016/j.ijbiomac.2022.09.260 (2022).
27. Xie, B. et al. Induction of autophagy and suppression of type I IFN secretion by CSFV. *Autophagy* **17**, 925–947. https://doi.org/10.1080/15548627.2020.1739445 (2021).
28. Xia, B. et al. Galactin-8 DNA methylation mediates macrophage autophagy through the MAPK/mTOR pathway to alleviate atherosclerosis. *Sci. Rep.* **15**, 603. https://doi.org/10.1038/s41598-024-85036-1 (2025).
29. Wang, A. et al. U0126 attenuates ischemia/reperfusion-induced apoptosis and autophagy in myocardium through MEK/ERK/EGR-1 pathway. *Eur. J. Pharmacol.* **788**, 280–285. https://doi.org/10.1016/j.ejphar.2016.06.038 (2016).
30. Oh, D. J., Lee, J. H., Kwon, Y. E. & Choi, H. M. Relationship between arteriovenous fistula stenosis and Circulating levels of neutrophil granule proteins in chronic Hemodialysis patients. *Ann. Vasc. Surg.* **77**, 226–235. https://doi.org/10.1016/j.avsg.2021.05.056 (2021).
31. Herman, A. B. et al. DPP4 Inhibition impairs senohemostasis to improve plaque stability in atherosclerotic mice. *J. Clin. Invest.* **133**. https://doi.org/10.1172/JCI165933 (2023).
32. Dace, D. S., Khan, A. A., Kelly, J. & Apte, R. S. Interleukin-10 promotes pathological angiogenesis by regulating macrophage response to hypoxia during development. *PLoS One* **3**, e3381. https://doi.org/10.1371/journal.pone.0003381 (2008).
33. Mandakhbayar, N. et al. Double hits with bioactive nanozyme based on cobalt-doped nanoglass for acute and diabetic wound therapies through anti-inflammatory and pro-angiogenic functions. *Bioact Mater.* **31**, 298–311. https://doi.org/10.1016/j.bioactmat.2023.08.014 (2024).
34. Ip, W. K. E., Hoshi, N., Shouval, D. S., Snapper, S. & Medzhitov, R. Anti-inflammatory effect of IL-10 mediated by metabolic reprogramming of macrophages. *Science* **356**, 513–519. https://doi.org/10.1126/science.aal3535 (2017).
35. Richter, F. C. et al. Adipocyte autophagy limits gut inflammation by controlling Oxylipin and IL-10. *EMBO J.* **42**, e112202. https://doi.org/10.15252/embj.2022112202 (2023).
36. Llorente-Cortés, V., Martínez-González, J. & Badimon, L. LDL receptor-related protein mediates uptake of aggregated LDL in human vascular smooth muscle cells. *Arterioscler. Thromb. Vasc Biol.* **20**, 1572–1579 (2000).
37. Li, H. et al. Lactoferrin induces the synthesis of vitamin B6 and protects HUVEC functions by activating PDXP and the PI3K/AKT/ERK1/2 pathway. *Int. J. Mol. Sci.* **20**. https://doi.org/10.3390/ijms20030587 (2019).
38. Li, F. et al. Blockade of CXCR4 promotes macrophage autophagy through the PI3K/AKT/mTOR pathway to alleviate coronary heart disease. *Int. J. Cardiol.* **392**, 131303. https://doi.org/10.1016/j.ijcard.2023.131303 (2023).
39. Hu, H. J. et al. PLK1 promotes cholesterol efflux and alleviates atherosclerosis by up-regulating ABCA1 and ABCG1 expression via the AMPK/PPARγ/LXRα pathway. *Biochim. Biophys. Acta Mol. Cell. Biol. Lipids.* **1867**, 159221. https://doi.org/10.1016/j.bbalip.2022.159221 (2022).
40. 40 Pi, S. et al. The P2RY12 receptor promotes VSMC-derived foam cell formation by inhibiting autophagy in advanced atherosclerosis. *Autophagy* **17**. https://doi.org/10.1080/15548627.2020.1741202 (2021).
41. Hao, T. et al. Phosphatidylethanolamine alleviates OX-LDL-induced macrophage inflammation by upregulating autophagy and inhibiting NLRP1 inflammasome activation. *Free Radic Biol. Med.* **208**, 402–417. https://doi.org/10.1016/j.freeradbiomed.2023.08.031 (2023).
42. Gao, F. et al. Orientin alleviates ox-LDL-induced oxidative stress, inflammation and apoptosis in human vascular endothelial cells by regulating sestrin 1 (SESN1)-mediated autophagy. *J. Mol. Histol.* **55**, 109–120. https://doi.org/10.1007/s10735-023-10176-z (2024).
43. Wu, M. et al. Bisphenol A impairs macrophages through inhibiting autophagy via AMPK/mTOR signaling pathway and inducing apoptosis. *Ecotoxicol. Environ. Saf.* **234**, 113395. https://doi.org/10.1016/j.ecoenv.2022.113395 (2022).
44. Guo, H. et al. Intermittent hypoxia-induced autophagy via AMPK/mTOR signaling pathway attenuates endothelial apoptosis and dysfunction in vitro. *Sleep. Breath.* **25**, 1859–1865. https://doi.org/10.1007/s11325-021-02297-0 (2021).
45. Carresi, C. et al. Oxidative stress triggers defective autophagy in endothelial cells: role in atherothrombosis development. *Antioxid. (Basel)* **10** https://doi.org/10.3390/antiox10030387 (2021).


## Acknowledgements

We would like to thank Chengfei Wang from Guizhou Medical University for histological assistance.

## Author contributions

BX and JL, Conceptualization; JL, methodology; JL, YL, and FL, software; JP and JD, validation; BX and PL, resources; JD and PL, data curation; JL, writing—original draft preparation; BX and PL, writing—review and editing; YL and JL, visualization; PL and BX, project administration; JW and CW, supervision; BX, funding acquisition; All authors reviewed the manuscript.

## Funding

This study was supported by National Natural Science Foundation of China (Grant No. 82460335).

## Declarations

## Competing interests

The authors declare no competing interests.

## Additional information

**Supplementary Information** The online version contains supplementary material available at https://doi.org/1

0.1038/s41598-025-95181-w.

**Correspondence** and requests for materials should be addressed to B.X. or P.L.